



Effect of Dy, Ho, and Er substitution on the magnetocaloric properties of Gd-Co-Al-Y high entropy bulk metallic glasses



C.M. Pang^a, L. Chen^a, H. Xu^a, W. Guo^a, Z.W. Lv^a, J.T. Huo^b, M.J. Cai^a, B.L. Shen^{a, **}, X.L. Wang^c, C.C. Yuan^{a, c, *}

^a School of Materials Science and Engineering, Jiangsu Key Laboratory for Advanced Metallic Materials, Southeast University, Nanjing, 211189, China

^b CAS Key Laboratory of Magnetic Materials and Devices, Ningbo Institute of Materials Technology & Engineering, Chinese Academy of Sciences, Ningbo, Zhejiang, 315201, China

^c Department of Physics, City University of Hong Kong, Kowloon, Hong Kong, China

ARTICLE INFO

Article history:

Received 9 December 2019

Received in revised form

27 January 2020

Accepted 28 January 2020

Available online 31 January 2020

Keywords:

High-entropy alloys
Magnetocaloric effect
Glass-forming ability
Metallic glasses

ABSTRACT

Glass-forming ability, thermal stability and magnetocaloric properties of Gd₂₅Co₂₅Al₂₅Y₂₅ and Gd₂₅Co₂₅Al₂₅Y₁₅RE₁₀ (RE = Dy, Ho, and Er) high entropy metallic glasses are evaluated. With the substitution of Y by adjacent heavy rare earth elements, i.e., Dy, Ho, or Er, the critical dimension (D_c), the width of the supercooled liquid region, magnetic entropy changes ($|\Delta S_M|$) and refrigeration capacity (RC) increase obviously. However, the magnetic transition temperature (T_C) almost keeps constant around 40 K, which may be attributed to the exchange interaction between Y and transition metal or other rare earth elements. Among resulting Gd₂₅Co₂₅Al₂₅Y₁₅RE₁₀ metallic glasses, the peak values of $|\Delta S_M|$ and RC can be improved from 6.76 to 7.35 Jkg⁻¹K⁻¹ and 424 to 488 Jkg⁻¹ when substituting Dy by Ho. This makes Gd₂₅Co₂₅Al₂₅Y₁₅Ho₁₀ as an attractive candidate for magnetic refrigerants in hydrogen liquefaction temperature range.

© 2020 Elsevier B.V. All rights reserved.

1. Introduction

The magnetocaloric effect (MCE) is intrinsic to magnetic materials, which is detected as the heating or the cooling of magnetic materials under a varying magnetic field. For the past decades, magnetic refrigerants with high MCE induced tremendous attention due to their potential industrial applications [1–3]. Compared with the conventional gas compression refrigeration, magnetic refrigeration has advantages of high energy efficiency and environmental friendliness. Incipiently, people usually focus on the familiar crystalline materials such as paramagnetic salt pills used in commissioning space cryogenic vacuum systems and Gd-Si-Ge alloys with giant magnetocaloric effects [4,5]. However, their range of magnetic transition temperature characterized by δT_{FWHM} is very narrow generally, which leads to a poor refrigeration capacity (RC) [5,6]. Thus, intensive efforts have been carried out for searching

magnetic refrigerants with large magnetic entropy change ($|\Delta S_M|$) and δT_{FWHM} of various temperature ranges [7–9].

Studies have proved that Gd-Co-Al amorphous materials have a relatively large $|\Delta S_M|$ and a board δT_{FWHM} in changing the magnetic field due to their special constituents together with disordered structure [10,11]. However, these alloys show a low glassy forming ability (GFA) and thermal stability, which severely restrain their potential applications [12–14]. According to previous reports, the addition of the Yttrium element would enhance GFA [15–17]. On the other hand, the mixture of multiple constitute elements can enlarge the configurational entropy [18] of high entropy (HE) alloy systems, which effectively enhances the thermal stability and mechanical strength [19–21]. Therefore, the HE bulk metallic glasses (MGs) based on Gd-Co-Al-Y alloy systems with equiatomic composition and a large configurational entropy may be desirable for the magnetic refrigeration.

Considering the previous studies on the magnetic and magnetocaloric properties of Gd_{65-2x}RE_xFe₂₀Al₁₅, Ho₂₀Er₂₀Co₂₀Al₂₀RE₂₀, and Er₂₀Dy₂₀Co₂₀Al₂₀RE₂₀ HE MGs, it can be summarized that the heavy REs in these materials may play the key role in the process of increasing $|\Delta S_M|$ due to their complex electronic structure [19–22]. Nevertheless, the variation of $|\Delta S_M|$ caused by adjacent heavy REs is

* Corresponding author. School of Materials Science and Engineering, Southeast University, China.

** Corresponding author.

E-mail addresses: blshen@seu.edu.cn (B.L. Shen), yuanchenchenneu@hotmail.com (C.C. Yuan).

not consistent in different compositions. For example, the maximum values of $|\Delta S_M|$ in Gd-Co-Al-RE systems increase with the substitution of Dy by Er, while the Gd-Fe-Al-Dy alloy system exhibits a larger $|\Delta S_M|$ than that of the same basic composition with Er addition [22–24]. Up to now, few works have investigated the influence of adjacent heavy REs on the magnetocaloric properties for Gd-Co-Al-Y HE bulk MGs, only some studies based on thermal stability and mechanical property, although the addition of RE is meaningful to enhance RC through tuning composition [21].

In this work, the $Gd_{25}Co_{25}Al_{25}Y_{25}$ and $Gd_{25}Co_{25}Al_{25}Y_{15}RE_{10}$ (RE = Dy, Ho, and Er) HE MGs were designed and prepared by using the copper mold casting method. The influence on GFA, thermal stability, and magnetocaloric properties based on the species of adjacent heavy REs (i.e., Dy, Ho, and Er) and their interplay was systematically investigated. This paper might shed new light on designing HE amorphous magnetic refrigeration materials with excellent properties and understanding their underneath mechanisms.

2. Experimental

Ingots with nominal compositions of $Gd_{25}Co_{25}Al_{25}Y_{25}$ and $Gd_{25}Co_{25}Al_{25}Y_{15}RE_{10}$ (RE = Dy, Ho, and Er) were first prepared by arc melting pure elements (above 99.9 wt. %) in a Ti-gettered argon atmosphere. Every ingot was remelted five times to ensure the homogeneity of composition in the sample. Glassy ribbons with an approximate width of 2 mm and thickness of 30 μm were prepared by a single roller melt spinning method. The as-cast rods with diameters of 1 mm were fabricated by the Cu mold suction casting method under the same argon atmosphere. The amorphous structure of melt-spun ribbons and the as-cast rods were ascertained by X-ray diffraction (XRD) with a Cu $K\alpha$ radiation ($2\theta = 15\text{--}80^\circ$). Thermal analysis was carried out by a differential scanning calorimeter (DSC) with a heating rate of 20 K/min by using the glassy ribbons and the MG rods with a diameter of about 1 mm. Field cooling magnetization (M_{FC}) of the ribbons was measured with an applied magnetic field of 200 Oe by a superconducting quantum interference device (SQUID) magnetometer (MPMS, Quantum Design) in the temperature range between 5 and 300 K. The isothermal magnetization ($M-H$) traces were measured with a varying magnetic field increasing from 0 to 50,000 Oe at diverse temperatures ranging from 10 to 130 K.

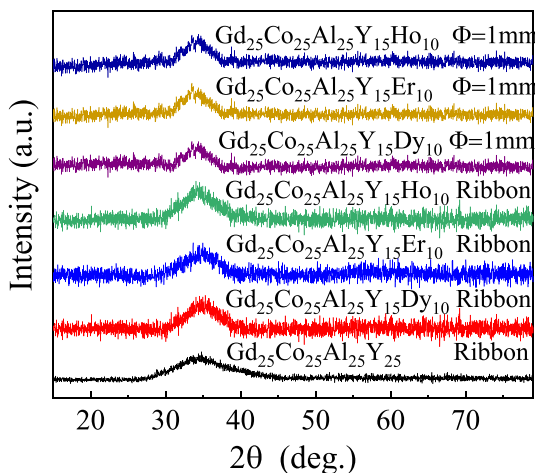


Fig. 1. XRD patterns of the $Gd_{25}Co_{25}Al_{25}Y_{25}$ and $Gd_{25}Co_{25}Al_{25}Y_{15}RE_{10}$ (RE = Dy, Ho, and Er) melt-spun ribbons and as-cast rods of 1 mm.

3. Results and discussion

Fig. 1 shows the XRD patterns of $Gd_{25}Co_{25}Al_{25}Y_{25}$ and $Gd_{25}Co_{25}Al_{25}Y_{15}RE_{10}$ (RE = Dy, Ho, and Er) melt-spun ribbons and as-cast rods with diameters of 1 mm. The typical broad humps without a sharp crystalline peak can be observed, which illustrates the fully glassy structure of these alloys. As seen in Fig. 1, the critical diameters of quinary $Gd_{25}Co_{25}Al_{25}Y_{15}RE_{10}$ (RE = Dy, Ho, and Er) are about 1 mm, while the composition of quaternary $Gd_{25}Co_{25}Al_{25}Y_{25}$ can only be made into a glassy ribbon with the thickness of around 30 μm . In comparison with the $Gd_{25}Co_{25}Al_{25}Y_{25}$ ribbon containing four elements in the equimolar ratio, the $Gd_{25}Co_{25}Al_{25}Y_{15}RE_{10}$ (RE = Dy, Ho, and Er) MGs have a better performance on the GFA. This may be attributed to the large discrepancy of atomic size between the HREs and other elements. i.e., Co, Al, and Y, where the negative heat of mixing enthalpy (ΔH_{mix}) among these alloys systems is similar which are shown in Fig. 2 [25].

The obvious endothermic reaction of $Gd_{25}Co_{25}Al_{25}Y_{25}$ and $Gd_{25}Co_{25}Al_{25}Y_{15}RE_{10}$ (RE = Dy, Ho, and Er) MGs due to the glass transition and the sharp exothermic peak related to crystallization are shown in Fig. 3, which further confirms the formation of the glassy structure for both $Gd_{25}Co_{25}Al_{25}Y_{25}$ ribbon and $Gd_{25}Co_{25}Al_{25}Y_{15}RE_{10}$ bulk MGs with a diameter of around 1 mm. The values of glass transition temperature (T_g), first crystallization temperature (T_x) and the supercooled liquid region ($\Delta T_x = T_x - T_g$) obtained from the DSC curves are listed in Table 1. Both T_g and T_x associated with thermal stability for supercooled liquids shift toward higher temperatures with the substitution of Y by the sequence of Er, Ho, and Dy elements. Just like the $p-d$ hybrid bonding [26–28] found in a metalloid-transition-metal system, here, the $4f$ shell of RE element may interact with the d shell of transition metal to form $f-d$ hybridization [29,30]. This hybridization phenomenon results in the localization of electrons and thereby a more stable state of system [26,29–31]. The reduction of the thermal stability may be attributed to the orbital hybridization process, which depends on the distinctive electron number of REs in the $4f$ shell (10, 11, and 12 for Dy, Ho, and Er, respectively). In reported quinary $Ho_{20}Er_{20}Co_{20}Al_{20}RE_{20}$ (RE = Gd, Dy, and Tm) [19], $Er_{20}Dy_{20}Co_{20}Al_{20}RE_{20}$ (RE = Gd, Tb, and Tm) [20], and quaternary $Gd_{25}Co_{25}Al_{25}RE_{25}$ (RE = Tb, Dy, and Ho) [12] HE MGs, it is found that both T_g and T_x increase in terms of the sequence of the adjacent heavy RE elements. It seems that more electrons in the $4f$ shell contribute to $f-d$ hybridization between transition metal element Co and heavy RE

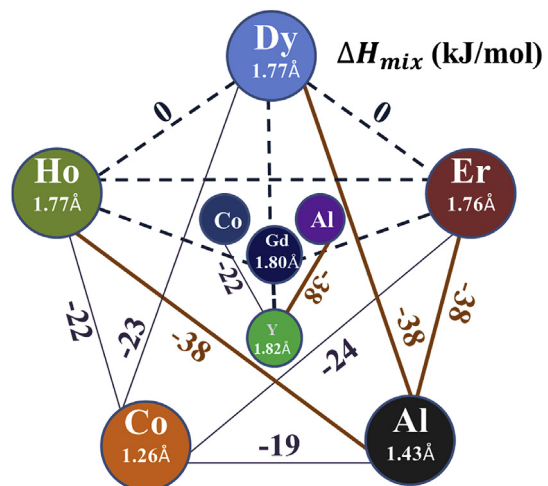


Fig. 2. The enthalpy of mixing (ΔH_{mix}) and atomic size of the constituent elements in $Gd_{25}Co_{25}Al_{25}Y_{25}$ and $Gd_{25}Co_{25}Al_{25}Y_{15}RE_{10}$ (RE = Dy, Ho, and Er) HE MGs.

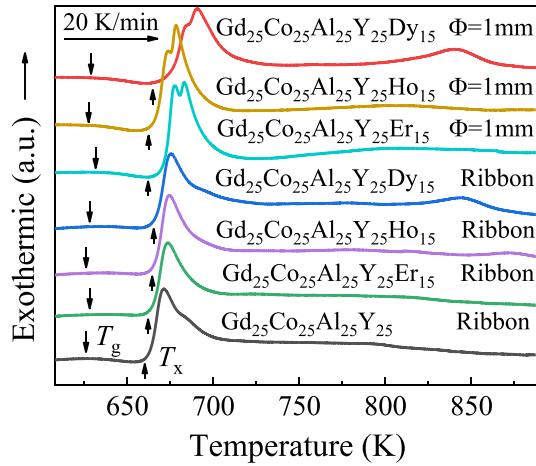


Fig. 3. DSC traces of the $Gd_{25}Co_{25}Al_{25}Y_{25}$ and $Gd_{25}Co_{25}Al_{25}Y_{15}RE_{10}$ (RE = Dy, Ho, and Er) melt-spun ribbons and as-cast rods of 1 mm.

elements. However, in our studied $Gd_{25}Co_{25}Al_{25}Y_{15}RE_{10}$ HE MG systems, T_g almost keeps constant of 626–628 K and T_x is reduced when substituting Y by the sequence of Dy, Ho, and Er according to their electron number in 4f orbital. These anomalies might be attributed to the strong interaction between Y and transition metal and/or other REs, where Y is a RE element with two 5s electrons and one 4d electron. We also find that the supercooled liquid region ($\Delta T_x = T_x - T_g$) of $Gd_{25}Co_{25}Al_{25}Y_{25}$ is around 36 K, which is quite narrow as compared with other $Gd_{25}Co_{25}Al_{25}RE_{25}$ (RE = Tb, Dy, and Ho) [12], seen in Table 1. It suggests that *d-d* direct exchange interaction [27,32] between Co and Y might lead to an unstable state of the $Gd_{25}Co_{25}Al_{25}Y_{25}$ supercooled liquid. However, with the substitution of Y by Dy, Ho, or Er, ΔT_x become slightly wider with the relatively higher T_x than that of quaternary $Gd_{25}Co_{25}Al_{25}Y_{25}$. This result shows that the addition of the fifth component actually improves the GFA not only relying on the atomic bonding but also influenced by the high stability of supercooling liquids due to four core effects proposed in HE alloys [18,21]. It indicates that the four core effects, i.e. high-entropy effect, sluggish diffusion effect, lattice-distortion effect, and cocktail effect, caused by the multi-component with different atom size and chemical interaction, play a dominant role in determining the formation of HE bulk MGs as well.

Fig. 4 shows the magnetization temperature curves of $M-T$ cool down to 5 K after heating up under the applied field of 200 Oe for $Gd_{25}Co_{25}Al_{25}Y_{25-x}RE_x$ ($x = 0, 10$; RE = Dy, Ho, and Er). The

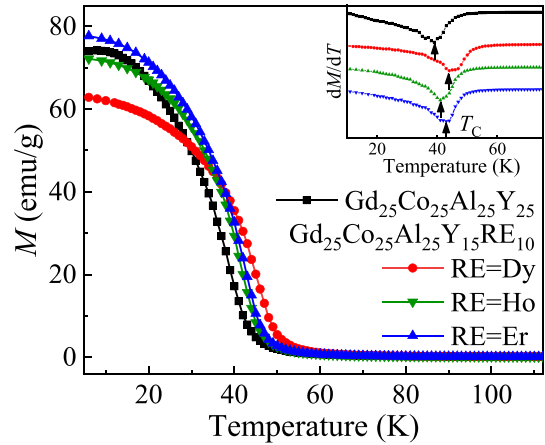


Fig. 4. Temperature dependence of FC magnetization under a magnetic field of 200 Oe for $Gd_{25}Co_{25}Al_{25}Y_{25}$ and $Gd_{25}Co_{25}Al_{25}Y_{15}RE_{10}$ (RE = Dy, Ho, and Er) MGs. The inset shows the curves of dM/dT versus temperature.

magnetization as a function of temperature decreases gradually, demonstrating an obvious magnetic transition from ferromagnetism to paramagnetism caused by the disorder of magnetic moment. Additionally, the values of magnetic transition temperature (T_C) defined by the minimum in the temperature dependence of dM/dT are 39, 44, 41, and 43 K for $Gd_{25}Co_{25}Al_{25}Y_{25-x}RE_x$ ($x = 0, 10$; RE = Dy, Ho, and Er) shown in the inset of Fig. 4, respectively. These values and their change as a function of composition are smaller than that of $Gd_{25}Co_{25}Al_{25}RE_{25}$ (RE = Tb, Dy, and Ho) [12] listed in Table 1. As suggested in the work of other HE MG systems, e.g. $Gd_{25}Co_{25}Al_{25}RE_{25}$ (RE = Tb, Dy, and Ho) [12], $Ho_{20}Er_{20}Co_{20}Al_{20}RE_{20}$ (RE = Gd, Dy, and Tm) [19], and $Er_{20}Dy_{20}Co_{20}Al_{20}RE_{20}$ (RE = Gd, Tb, and Tm) [20], T_C consists well with the trend of de Gennes factor (G) under the frame of Rudermann-Kittel-Kasuya-Yosida (RKKY) indirect interaction theory [12,19,20,33]. Here, G can be expressed as [34]:

$$G = J(J+1)(g-1)^2 \quad (1)$$

where J is the total orbital quantum number and g the gyromagnetic ratio. g can be expressed as $g = 1 + [J(J+1) + S(S+1) - L(L+1)] / 2J(J+1)$, where S is the spin quantum number and L the orbital angular momentum quantum number. Whereas for the $Gd_{25}Co_{25}Al_{25}Y_{15}RE_{10}$ (RE = Dy, Ho, and Er) systems studied here, with decreasing G (the theoretically predicted values of G are 7.08, 4.5, and 2.55 for Dy, Ho, and Er, respectively), T_C nearly lies in a

Table 1

The glass transition temperature (T_g), crystallization temperature (T_x), supercooled liquid region ($\Delta T_x = T_x - T_g$), Curie temperature (T_C), maximum magnetic entropy change (ΔS_M^{pk}), full width at half maximum magnetic entropy change (δT_{FWHM}), refrigeration capacity (RC), n and N are exponents in the equations of $|\Delta S_M^{pk}| \propto H^n$ and $RC \propto H^N$ under a magnetic field of 5 T of $Gd_{25}Co_{25}Al_{25}Y_{25}$ and $Gd_{25}Co_{25}Al_{25}Y_{15}RE_{10}$ (RE = Dy, Ho, and Er) glassy alloys.

Composition	T_g (K)	T_x (K)	ΔT_x (K)	$ \Delta S_M^{pk} $ (Jkg ⁻¹ K ⁻¹)	δT_{FWHM} (K)	RC (Jkg ⁻¹)	T_C (K)	n	N	Ref.
$Gd_{25}Co_{25}Al_{25}Y_{25}$	626	662	36	6.02	68.67	413	39	0.79	1.01	This work
$Gd_{25}Co_{25}Al_{25}Y_{15}Dy_{10}$	628	666	38	6.76	62.75	424	44	0.86	1.16	This work
$Gd_{25}Co_{25}Al_{25}Y_{15}Ho_{10}$	626	665	39	7.35	66.32	488	41	0.84	1.13	This work
$Gd_{25}Co_{25}Al_{25}Y_{15}Er_{10}$	628	664	36	6.96	68.49	477	43	0.82	1.03	This work
Gd	–	–	–	9.8	–	–	293	–	–	[6]
$Gd_5Si_2Ge_2$	–	–	–	18.6	16.45	306	276	–	–	[1]
$Gd_{35}Co_{20}Al_{25}$	562.5	629	66.5	9	88.9	800	112	–	–	[8]
$Gd_{25}Co_{25}Al_{25}Tb_{25}$	612	659	47	8.88	65	577	73	0.75	–	[12]
$Gd_{25}Co_{25}Al_{25}Dy_{25}$	627	669	42	8.72	65	567	60	0.74	–	[12]
$Gd_{25}Co_{25}Al_{25}Ho_{25}$	633	675	42	9.78	64	626	50	0.77	–	[12]
$Gd_{55}Co_{25}Al_{20}$	–	–	–	9.1	87.8	799	113	0.81	–	[40]
$Dy_{50}Gd_7Co_{23}Al_{20}$	–	–	–	9.77	29.7	290	26	0.86	–	[41]
$Ho_{20}Er_{20}Co_{20}Al_{20}Gd_{20}$	612	652	40	11.2	56	627	37	0.85	1.12	[19]

small temperature region around 40 K. This might be influenced by the addition of Y in $\text{Gd}_{25}\text{Co}_{25}\text{Al}_{25}\text{Y}_{25-x}\text{RE}_x$ systems. As seen in Table 1 that T_C of $\text{Gd}_{25}\text{Co}_{25}\text{Al}_{25}\text{Y}_{25}$ is only 39 K, which is almost a half of 73 K that reported for $\text{Gd}_{25}\text{Co}_{25}\text{Al}_{25}\text{Tb}_{25}$ in the studies of $\text{Gd}_{25}\text{Co}_{25}\text{Al}_{25}\text{RE}_{25}$ (RE = Tb, Dy, and Ho) HE MGs [12]. It indicates that T_C is more affected by Y due to the less RKKY effects in $\text{Gd}_{25}\text{Co}_{25}\text{Al}_{25}\text{Y}_{25}$ for the lack of 4f shells in Y.

Fig. 5 taking $\text{Gd}_{25}\text{Co}_{25}\text{Al}_{25}\text{Y}_{15}\text{Ho}_{10}$ as an example shows a set of isothermal magnetization curves at different temperatures. The temperature steps of 5 K were chosen in the vicinity of the T_C , and step of 10 K for the region far away from T_C . The scanning speed is low enough to ensure isothermal state of alloys which is easily influenced by the demagnetization factor. The magnetization intensity increases sharply and reaches saturation rapidly below the T_C , while it becomes a straight line gradually above the T_C , showing an obvious magnetic transition from the ferromagnetic to paramagnetic behavior. Fig. 6 shows the diagram of $\text{Gd}_{25}\text{Co}_{25}\text{Al}_{25}\text{Y}_{15}\text{Ho}_{10}$ between 10 and 130 K, and the temperature of 10, 50, and 90 K is elected, respectively. The transition with a negative slope is considered as a first-order magnetic transition; otherwise, the positive slope stands for a second-order magnetic phase transition. Obviously, $\text{Gd}_{25}\text{Co}_{25}\text{Al}_{25}\text{Y}_{15}\text{Ho}_{10}$ exhibits a typical second-order magnetic transition. From the above curves, it is clear that a large MCE characterized by RC can be observed near T_C when the magnetization varies sharply in a constant field.

The $|\Delta S_M|$ and the full width of half maximum of magnetic entropy change (δT_{FWHM}) are two pivotal parameters to evaluate the RC according to Gschneidner method [35], which can be expressed as:

$$\text{RC} = |\Delta S_M^{\text{pk}}| \times \delta T_{FWHM} \quad (2)$$

In the isothermal process of magnetization, the $|\Delta S_M|$ can be given by integrating the Maxwell relation over the magnetic field [36]:

$$\Delta S_M(T, H) = \Delta S_M(T, H) - S_M(T, 0) - \int_{H_0}^{H_{\text{max}}} \left(\frac{\partial M}{\partial T} \right) dH \quad (3)$$

Where H_{max} and H_0 represent the maximum and minimum of the applied magnetic field. Maximal value of 5 T was used in our work. Combined with equations (2) and (3), the RC could be calculated

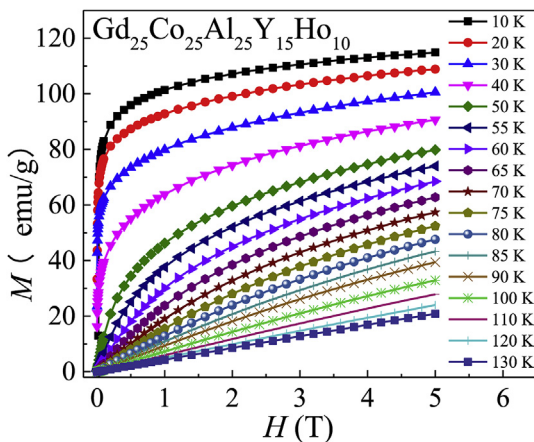


Fig. 5. The isothermal magnetization curves for the as-cast $\text{Gd}_{25}\text{Co}_{25}\text{Al}_{25}\text{Y}_{15}\text{Ho}_{10}$ HE MG measured at the temperatures between 10 and 130 K. Temperature intervals of 5 K for 50–90 K and 10 K for 10–50 K and 90–130 K, respectively.

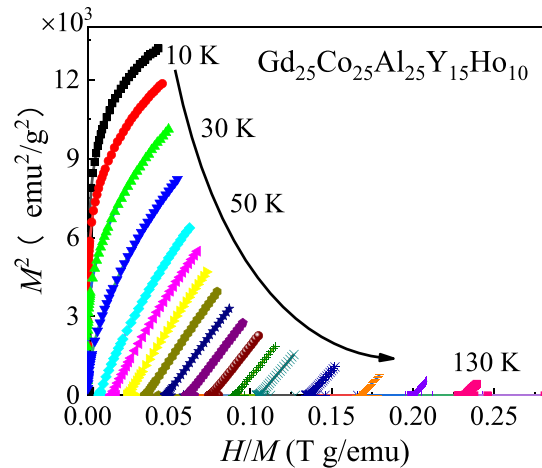


Fig. 6. Arrott plots for the as-cast $\text{Gd}_{25}\text{Co}_{25}\text{Al}_{25}\text{Y}_{15}\text{Ho}_{10}$ HE MG measured at the temperatures between 10 and 130 K.

quantitatively to evaluate the magnetocaloric properties of HE MGs in the work.

Fig. 7 shows the temperature dependence of $|\Delta S_M|$ of the $\text{Gd}_{25}\text{Co}_{25}\text{Al}_{25}\text{Y}_{25-x}\text{RE}_x$ ($x = 0, 10$; RE = Dy, Ho, and Er) HE MGs under the applied magnetic field of 5 T. It is noteworthy that the peak values of $|\Delta S_M|$ ($|\Delta S_M^{\text{pk}}|$) are 6.76, 7.35, and 6.96 $\text{J kg}^{-1}\text{K}^{-1}$ respectively for the MGs with RE = Dy, Ho, and Er, showing their excellent MCE. Meanwhile, the effect of substitution of the Y element on magnetocaloric properties has been shown in Fig. 8. Combined with $|\Delta S_M|$ -T curves, we find that the values of δT_{FWHM} are 63, 66, and 68 K under an applied magnetic field of 5 T for Dy, Ho, and Er substituted HE MGs. Additionally, the RC values for these HE MGs are 424, 488, and 477 $\text{J kg}^{-1}\text{K}^{-1}$ with RE = Dy, Ho, and Er, respectively, which are much larger than that of quaternary $\text{Gd}_{25}\text{Co}_{25}\text{Al}_{25}\text{Y}_{25}$. It is noted that $\text{Gd}_{25}\text{Co}_{25}\text{Al}_{25}\text{Y}_{15}\text{Ho}_{10}$ HE bulk MG has the largest $|\Delta S_M^{\text{pk}}|$ and RC among these three alloys. While the δT_{FWHM} of $\text{Gd}_{25}\text{Co}_{25}\text{Al}_{25}\text{Y}_{15}\text{Er}_{10}$ alloy is the widest. It agrees well with the observation in quaternary $\text{Gd}_{25}\text{Co}_{25}\text{Al}_{25}\text{RE}_{25}$ (RE = Tb, Dy, and Ho) HE MGs, where the composition with RE = Ho exhibits the largest $|\Delta S_M^{\text{pk}}|$ and RC among these three alloys [12]. Cocktail effects in the HE MGs result in a strong chemical effect on the properties [18]. In addition to the contribution from the entropy of mixing

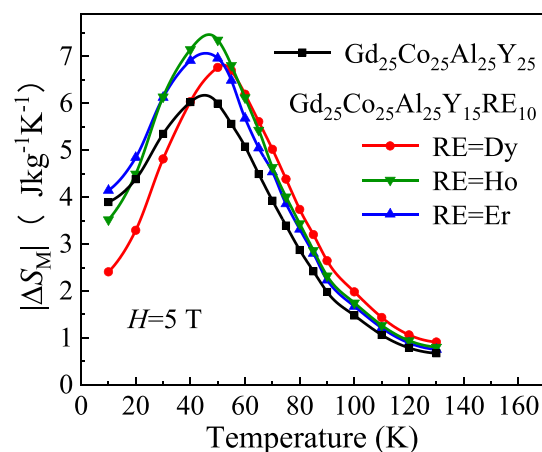


Fig. 7. The magnetic entropy change ($|\Delta S_M|$) as a function of temperature under 5 T for $\text{Gd}_{25}\text{Co}_{25}\text{Al}_{25}\text{Y}_{25}$ and $\text{Gd}_{25}\text{Co}_{25}\text{Al}_{25}\text{Y}_{15}\text{RE}_{10}$ (RE = Dy, Ho, and Er) HE MGs.

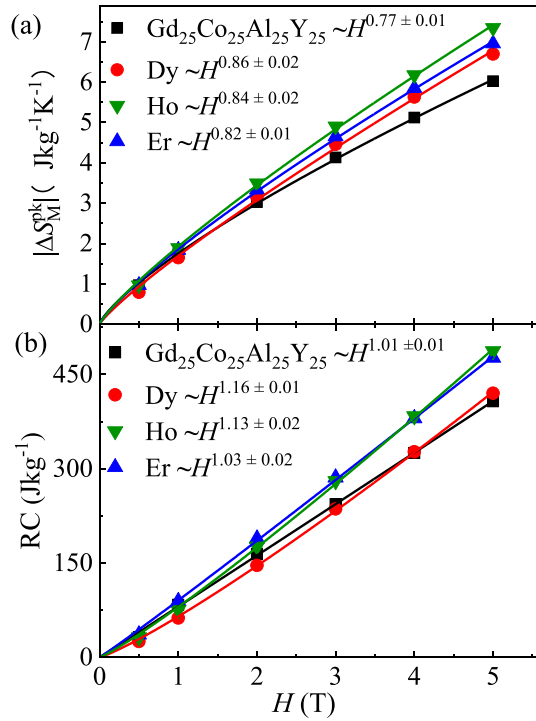


Fig. 8. Magnetic field dependence of (a) peak values of magnetic entropy changes ($|\Delta S_M^{pk}|$), and (b) RC as a function of the applied magnetic field for $Gd_{25}Co_{25}Al_{25}Y_{25}$ and $Gd_{25}Co_{25}Al_{25}Y_{15}RE_{10}$ (RE = Dy, Ho, and Er) MGs. The solid lines are fitting curves of $|\Delta S_M^{pk}| \propto H^n$ and $RC \propto H^N$ with standard errors, respectively.

atomic configuration (ΔS_{config}), the main effect of RKKY interaction between the magnetic elements might be reduced due to the influence of multicomponent in HE alloy systems. The $|\Delta S_M^{pk}|$ and RC are more dependent on the theoretical magnetic entropy (S_M) associated with the magnetic ordering process. The theoretical molar magnetic entropy can be given by the equation [37]:

$$S_M = R \ln(2J + 1) \quad (4)$$

It is found that the value of S_M for Ho ($S_M = 23.6 \text{ J mol}^{-1} \text{ K}^{-1}$) is slightly larger than that of Dy ($S_M = 23.0 \text{ J mol}^{-1} \text{ K}^{-1}$) and Er ($S_M = 23.0 \text{ J mol}^{-1} \text{ K}^{-1}$), which well explains the fact that the $Gd_{25}Co_{25}Al_{25}Y_{15}Ho_{10}$ has the largest $|\Delta S_M^{pk}|$ and RC but not contains the largest electron numbers in 4f shells that contributes to the relatively strong RKKY indirect interaction.

According to the previous experimental results and theoretical analysis, the magnetocaloric properties of second-order magnetic transition materials show a distinct dependency of the applied magnetic field in the vicinity of T_C [38]. The relationship between the magnetic field and $|\Delta S_M^{pk}|$, as well as RC, can be expressed as power-law based on a mean-field theory picture [39]: $|\Delta S_M^{pk}| \propto H^n$ and $RC \propto H^N$, where n and N are exponents influenced by critical exponents of alloy systems, respectively. These exponents can be evaluated through the fitting curves data in Fig. 8 (a) and 8 (b). In general, $n = 1$ at the temperature below the T_C ; $n = 2$ in the paramagnetic range of temperature results from the Curie-Weiss law for soft magnetic MGs materials [39]. However, in this work, for the quaternary $Gd_{25}Co_{25}Al_{25}Y_{25}$ HE MG: $n = 0.77 \pm 0.01$, and $N = 1.01 \pm 0.01$; for the quinary $Gd_{25}Co_{25}Al_{25}Y_{15}RE_{10}$ HE MGs, RE = Dy: $n = 0.86 \pm 0.02$, and $N = 1.16 \pm 0.01$; RE = Ho: $n = 0.84 \pm 0.02$, and $N = 1.13 \pm 0.02$; RE = Er: $n = 0.82 \pm 0.01$, and

$N = 1.03 \pm 0.02$. The exponent n of the quaternary $Gd_{25}Co_{25}Al_{25}Y_{25}$ HE MG is similar to the values of other reported quaternary $Gd_{25}Co_{25}Al_{25}RE_{25}$ (RE = Tb, Dy, and Ho) ($n \sim 0.75, 0.75$, and 0.77) HE MGs [12], indicating that the composition with Y element addition exhibits a similar magnetic field dependence as other systems. Compared with the above quaternary alloy systems, the exponents n of quinary $Gd_{25}Co_{25}Al_{25}Y_{15}RE_{10}$ (RE = Dy, Ho, and Er) HE MGs are slightly larger, which are more close to the Gd-based ($n \sim 0.81$) and Dy-based ($n \sim 0.86$) MGs [40,41]. Moreover, all exponents n of our studied systems deviate from the predicted value ($n \sim 2/3$) based on mean-field theory [42] which may be attributed to the neglected fluctuations and heterogeneities of microstructures for MGs [41]. The core effects shown by HE alloys like high entropy and cocktail effects [18,21] may promote such structural fluctuations and heterogeneities, which effectively improves magnetocaloric properties of quinary $Gd_{25}Co_{25}Al_{25}Y_{15}RE_{10}$ alloy systems. It is also noticed that the $Gd_{25}Co_{25}Al_{25}Y_{15}Dy_{10}$ have the largest exponents n and N , which leads to the rapid increase of $|\Delta S_M^{pk}|$ and RC with the variation of the applied magnetic field. As a result, this alloy will exhibit excellent property as refrigerants under a changing magnetic field.

In this work, the high thermal stability and the improved magnetocaloric property can be achieved by the heavy REs (RE = Dy, Ho, and Er) substitution in $Gd_{25}Co_{25}Al_{25}Y_{15}RE_{10}$. Based on DSC results, the wider supercooled liquid region accompanied by the complex crystallization behaviors of quinary $Gd_{25}Co_{25}Al_{25}Y_{15}RE_{10}$ (RE = Dy, Ho, and Er) bulk MGs has been observed. Comparing with the quaternary $Gd_{25}Co_{25}Al_{25}Y_{25}$ ribbon sample, the main endothermic peaks split into two peaks for $Gd_{25}Co_{25}Al_{25}Y_{15}RE_{10}$ rods with diameters of 1 mm as shown in Fig. 3, indicating better thermal stability of $Gd_{25}Co_{25}Al_{25}Y_{15}RE_{10}$ bulk MGs. It might be due to the formation of complex chemical short- or medium-range-ordering configurations in RE-added systems [43,44]. On the other hand, the large atomic size of RE elements makes the long-range atomic rearrangement become more difficult. Besides, the larger degree of configurational disorders induced by high-entropy effects further hinders atomic diffusion [18,21], which also leads to the high thermal stability of quinary $Gd_{25}Co_{25}Al_{25}Y_{15}RE_{10}$ in the supercooled liquid region. The improvement of GFA and thermal stability upon RE element addition has been reported in other MGs as well, such as Fe–Nb–B [43,44]. It is found that only 5 at. % Ho addition in $Fe_{66}Ho_5Nb_6B_{23}$ causes the increase of supercooled liquid region from 48 to 90 K as well as the competitive crystallization behaviors demonstrated by multiple endothermic peaks in DSC curves [43]. The appearance of abnormal endothermic peaks in the supercooled liquid region due to the structural rearrangement of the metastable configuration with a strong chemical short- or medium-range order induced by RE element is suggested to be closely related to the super-high thermal stability of Fe–Nb–B–RE MG systems [43,44]. However, such abnormal endothermic peaks have not been observed in our studied $Gd_{25}Co_{25}Al_{25}Y_{15}RE_{10}$ systems, which is consistent with the relatively narrow ΔT_x of $Gd_{25}Co_{25}Al_{25}Y_{15}RE_{10}$ (~ 40 K) as compared to that of $Fe_{66}Ho_5Nb_6B_{23}$ bulk MGs (~ 90 K).

We also find that when substituting Y by adjacent heavy RE elements, both magnetic entropy changes ($|\Delta S_M|$) and refrigeration capacity (RC) increase obviously, in virtue of the large theoretical molar magnetic entropy S_M , the strong RKKY indirect interaction, and the pronounced structural fluctuations/ heterogeneities in RE added systems. However, the magnetic transition temperature, T_C , almost keeps a constant of about 40 K. It has been proposed that regardless of the contribution of the crystalline electric field, there are three main factors that may influence the magnetocaloric property of MGs near the T_C [37], i.e., the theoretical magnetic entropy S_M , the G , and the RKKY interaction. Due to little direct

overlap of 4*f* electron wave functions between the lanthanide metals, the magnetic coupling occurs from the polarization of the 4*f* electrons on adjacent lanthanide atoms via the conductive 6*s* electrons. Therefore, the T_C is mainly associated with the indirect interaction between the atoms, where the *G* based on RKKY theory plays a key role [12,20,33]. It can be shown in Fig. 9(a) that the T_C indeed accords well with the *G* with the variation of heavy RE elements in previously studied HE MGs, such as $Gd_{25}Co_{25}Al_{25}RE_{25}$ [12], $Er_{20}Dy_{20}Co_{20}Al_{20}RE_{20}$ [19], and $Ho_{20}Er_{20}Co_{20}Al_{20}RE_{20}$ [20]. However, the T_C of $Gd_{25}Co_{25}Al_{25}Y_{15}RE_{10}$ (RE = Dy, Ho, and Er) MGs doesn't change as a function of composition, keeping a value of about 40 K similar to that of $Gd_{25}Co_{25}Al_{25}Y_{25}$, which seems quite different from the expectation of previous works. One possible reason for the abnormal trend of T_C is attributed to the weakened *f-f* exchange interaction owing to the lack of heavy RE elements in Y added systems. It is reported that the RE and RE (R-R) exchange interaction induced by 4*f* electrons dominates the value of T_C in RE-based alloy systems. Normally, the substitution of RE with lower *G* can result in a decrease in T_C [12,20,45]. For example, in RFe_3 intermetallic compounds, due to the fact that the *G* value of Y element is zero, the T_C of YFe_3 is lowest among all $REFe_3$ [45]. Thus, in our studied MG systems, with the addition of 25 at.% Y, T_C of $Gd_{25}Co_{25}Al_{25}Y_{25}$ HE MG (39 K) is reduced about 34 K as compared with $Gd_{25}Co_{25}Al_{25}Tb_{25}$ HE MG (73 K). Generally, the magnetic transition from the ferromagnetism to paramagnetism is as a result of the competition between the magnetic coupling and thermal effect dominated by temperature. When we substitute Y by 10 at.% heavy RE, the remaining 15 at.% Y strongly weakens the magnetic exchange interaction between RE and RE, where the thermal effect is more dominant during the magnetic ordering transition. Therefore, although *G* of Dy, Ho, and Er are quite different from each other as shown in Fig. 9 (a), in our studied $Gd_{25}Co_{25}Al_{25}Y_{15}RE_{10}$ (RE = Dy, Ho, and Er) MG systems, the value of T_C still keeps a constant close to that of $Gd_{25}Co_{25}Al_{25}Y_{25}$ MG.

Actually, the Y element has a significant impact on T_C of RE-based MG, which effectively reduces T_C for lack of 4*f*-4*f* interactions. As shown in Fig. 9 (b), compared with Gd-Tb-Dy-Al-M (M = Fe) [46], the values of T_C for MGs with Y addition such as $Gd_{25}Co_{25}Al_{25}Y_{25}$ and $Gd_{25}Co_{25}Al_{25}Y_{15}RE_{10}$ (RE = Dy, Ho, and Er) is relatively smaller. While in $Gd_{25}Co_{25}Al_{25}RE_{25}$ [12] MGs, with the substitution of Y by Ho, Dy, and Tb, the T_C increases gradually. It also can be seen in Fig. 9 (b) that less Y addition of 5 at.% may respond to the increase of the T_C of $Gd_{36}Co_{20}Al_{24}Y_{20}$ MGs ($T_C = 53$ K) [47] about

14 K as compared with $Gd_{25}Co_{25}Al_{25}Y_{25}$ ($T_C = 39$ K). These phenomena imply that the indirect exchange interaction between 4*f* and 4*f* electrons plays an important role in determining the T_C of RE-based alloys. Besides, the 3*d*-4*f* interaction, as well as 3*d*-3*d* interaction, also relates to the T_C for magnetic ordering transition [45]. For instance, in Gd-Tb-Dy-Al-M (M = Fe, Co, and Ni) HE MGs [46], the strong RE and transition metal magnetic interaction of RE and Fe (3 *d*⁶) as compared with that of Co (3 *d*⁷) leads to a higher value of T_C . Therefore, based on the above knowledge, the value of T_C can be easily tuned to satisfy the application of RE-based HE MGs as magnetic refrigerants in various temperature ranges, especially for the hydrogen liquefaction temperature range.

4. Conclusion

$Gd_{25}Co_{25}Al_{25}Y_{25}$ and $Gd_{25}Co_{25}Al_{25}Y_{15}RE_{10}$ (RE = Dy, Ho, and Er) HE MGs were studied in this work, which exhibit the tunable magnetocaloric properties and the GFA with the substitution of Y by heavy RE elements Dy, Ho, or Er. The following are the concluded main results:

- (1) The substitution of heavy REs including Dy, Ho, or Er improves the GFA and thermal stability of the quaternary $Gd_{25}Co_{25}Al_{25}Y_{25}$ alloy, which is not only relying on the strong atomic bonding and the large discrepancy of atomic size but also due to four core effects introduced by multicomponent in HE MGs.
- (2) It is particular noting that the T_C (44, 41, and 43 K) nearly keep constant around 40 K with the substitutional sequence of Dy, Ho, and Er for $Gd_{25}Co_{25}Al_{25}Y_{15}RE_{10}$ HE MGs, which is distinguished with the normal observations in other HE MGs, where T_C shows a positive relationship with de Gennes factor (*G*). This indicates that T_C is more influenced by Y in $Gd_{25}Co_{25}Al_{25}Y_{15}RE_{10}$ HE MGs due to the less RKKY effects in $Gd_{25}Co_{25}Al_{25}Y_{25}$ for the lack of 4*f* orbital in Y.
- (3) The $Gd_{25}Co_{25}Al_{25}Y_{15}RE_{10}$ (RE = Dy, Ho, and Er) HE bulk MGs present a typical second-order magnetic transition from ferromagnetism to paramagnetism. Among the three HE bulk MGs, the composition of $Gd_{25}Co_{25}Al_{25}Y_{15}Ho_{10}$ shows the largest values of $|\Delta S_M|$ and RC of up to 7.35 $Jkg^{-1}K^{-1}$ and 488 Jkg^{-1} , which are larger than those of many crystalline and amorphous magnetic refrigerants.

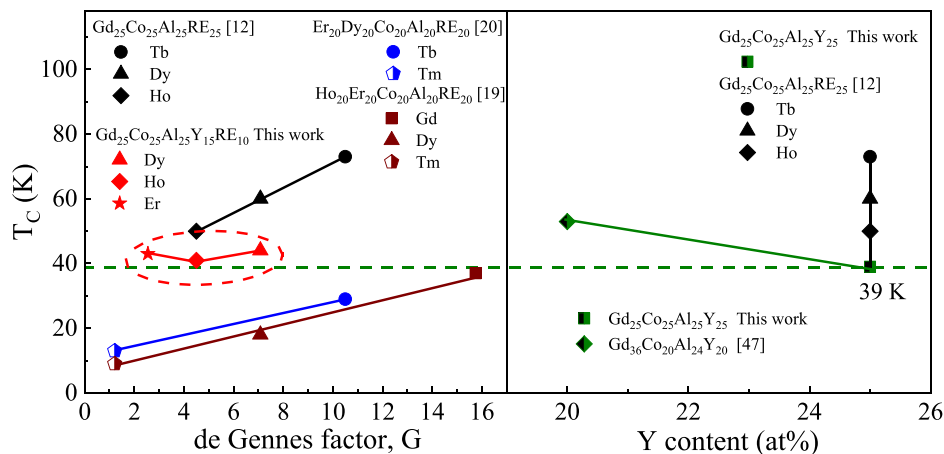


Fig. 9. Curie temperature T_C as a function of (a) de Gennes factor *G* and (b) Y content for the $Gd_{25}Co_{25}Al_{25}Y_{25}$ and $Gd_{25}Co_{25}Al_{25}Y_{15}RE_{10}$ (RE = Dy, Ho, and Er) HE MGs in this work together with other HE MGs.

- (4) The $Gd_{25}Co_{25}Al_{25}Y_{15}Dy_{10}$ exhibits the largest exponents n (0.86) and N (1.16) among four studied HE MG systems, which leads to the excellent magnetocaloric properties under a changing magnetic field. This may be attributed to the structural fluctuations heterogeneities introduced by the high entropy effect in this system.

Declaration of competing interest

The authors declared that they have no conflicts of interest to this work. We declare that we do not have any commercial or associative interest that represents a conflict of interest in connection with the work submitted.

Credit authorship contribution statement

C.M. Pang: Methodology, Software, Investigation, Data curation, Visualization, Writing - original draft. **L. Chen:** Investigation. **H. Xu:** Investigation. **W. Guo:** Investigation. **Z.W. Lv:** Methodology, Software. **J.T. Huo:** Writing - review & editing. **M.J. Cai:** Methodology. **B.L. Shen:** Writing - review & editing, Project administration, Funding acquisition. **X.L. Wang:** Writing - review & editing. **C.C. Yuan:** Conceptualization, Investigation, Data curation, Visualization, Writing - original draft, Writing - review & editing, Project administration, Funding acquisition, Supervision.

Declaration of competing interest

The authors declared that they have no conflicts of interest to this work. We declare that we do not have any commercial or associative interest that represents a conflict of interest in connection with the work submitted.

Acknowledgements

This work was supported by the National Natural Science Foundation of China (Grant Nos. 51601038 and 51631003), the Natural Science Foundation of Jiangsu Province, China (Grant No. BK20171354), Jiangsu Key Laboratory for Advanced Metallic Materials (Grant No. BM2007204).

References

- V.K. Pecharsky, K.A. Gschneidner, Giant magnetocaloric effect in $Gd_5(Si_2Ge_2)$, *Phys. Rev. Lett.* 78 (1997) 4494–4497.
- H. Wada, Y. Tanabe, K. Hagiwara, M. Shiga, Magnetic phase transition and magnetocaloric effect of $DyMn_2Ge_2$, *J. Magn. Magn. Mater.* 218 (2000) 203–210.
- M.H. Yu, Y. Janssen, O. Tegus, J.C.P. Klaasse, Z.D. Zhang, E. Bruck, F.R. de Boer, K.H.J. Buschow, Crystal-field analysis of the magnetic properties measured on a $Ho_2Co_{15}Si_2$ single crystal, *Phys. Rev. B* 65 (2002) 224409.
- C. Hagmann, D.J. Benford, P.L. Richards, Paramagnetic salt pill design for magnetic refrigerators used in-space applications, *Cryogenics* 34 (1994) 213–219.
- V.K. Pecharsky, K.A. Gschneidner, $Gd_5(Si_xGe_{1-x})_2$: an extremum material, *Adv. Mater.* 13 (2001) 683–686.
- V.K. Pecharsky, K.A. Gschneidner, Magnetocaloric effect and magnetic refrigeration, *J. Magn. Magn. Mater.* 200 (1999) 44–56.
- K. Wu, C. Liu, Q. Li, J. Huo, M. Li, C. Chang, Y. Sun, Magnetocaloric effect of $Fe_{25}Co_{25}Ni_{25}Mo_5P_{10}B_{10}$ high-entropy bulk metallic glass, *J. Magn. Magn. Mater.* 489 (2019) 165404.
- S. Lu, M.B. Tang, L. Xia, Excellent magnetocaloric effect of a $Gd_{55}Al_{20}Co_{25}$ bulk metallic glass, *Phys. Rev. B Condens. Matter* 406 (2011) 3398–3401.
- F. Hu, Q. Luo, B. Shen, Thermal, magnetic and magnetocaloric properties of $FeErNb$ metallic glasses with high glass-forming ability, *J. Non-Cryst. Solids* 512 (2019) 184–188.
- J. Du, Q. Zheng, Y.B. Li, Q. Zhang, D. Li, Z.D. Zhang, Large magnetocaloric effect and enhanced magnetic refrigeration in ternary Gd-based bulk metallic glasses, *J. Appl. Phys.* 103 (2008), 023918.
- D. Chen, A. Takeuchi, A. Inoue, Thermal stability and mechanical properties of Gd-Co-Al bulk glass alloys, *Trans. Nonferrous Metal. Soc.* 17 (2007) 1220–1224.
- L. Xue, L. Shao, Q. Luo, B. Shen, $Gd_{25}RE_{25}Co_{25}Al_{25}$ (RE = Tb, Dy and Ho) high-entropy glassy alloys with distinct spin-glass behavior and good magnetocaloric effect, *J. Alloys Compd.* 790 (2019) 633–639.
- F. Canepa, M. Napolitano, M.L. Fornasini, F. Merlo, Structure and magnetism of Gd_2Co_2Ga , Gd_2Co_2Al and $Gd_{14}Co_3In_{2.7}$, *J. Alloys Compd.* 345 (2002) 42–49.
- C. Wu, D. Ding, L. Xia, Effect of Al addition on the glass-forming ability and magnetic properties of a Gd-Co binary amorphous alloy, *Chin. Phys. Lett.* 33 (2016), 016102.
- J. Kastil, J. Kamarad, P. Javorsky, Magnetocaloric effect of $Gd_{64}Co_{26}Al_9Y_1$ metallic glass, *J. Alloys Compd.* 545 (2012) 1–4.
- T. Bitoh, D. Watanabe, Effect of Yttrium addition on glass-forming ability and magnetic properties of Fe-Co-B-Si-Nb bulk metallic glass, *Metals* 5 (2015) 1127–1135.
- S. Lu, S. Sun, K. Li, H. Li, X. Huang, G. Tu, The effect of Y addition on the crystallization behaviors of Zr-Cu-Ni-Al bulk metallic glasses, *J. Alloys Compd.* 799 (2019) 501–512.
- Y. Zhang, T.T. Zuo, Z. Tang, M.C. Gao, K.A. Dahmen, P.K. Liaw, Z.P. Lu, Microstructures and properties of high-entropy alloys, *Prog. Mater. Sci.* 61 (2014) 1–93.
- J. Huo, L. Huo, J. Li, H. Men, X. Wang, A. Inoue, C. Chang, J.-Q. Wang, R.-W. Li, High-entropy bulk metallic glasses as promising magnetic refrigerants, *J. Appl. Phys.* 117 (2015), 073902.
- J. Li, L. Xue, W. Yang, C. Yuan, J. Huo, B. Shen, Distinct spin glass behavior and excellent magnetocaloric effect in $Er_{20}Dy_{20}Co_{20}Al_{20}RE_{20}$ (RE = Gd, Tb and Tm) high-entropy bulk metallic glasses, *Intermetallics* 96 (2018) 90–93.
- J. Kim, H.S. Oh, J. Kim, C.W. Ryu, G.W. Lee, H.J. Chang, E.S. Park, Utilization of high entropy alloy characteristics in Er-Gd-Y-Al-Co high entropy bulk metallic glass, *Acta Mater.* 155 (2018) 350–361.
- Y.K. Fang, H.C. Chen, C.C. Hsieh, H.W. Chang, X.G. Zhao, W.C. Chang, W. Li, Structures and magnetocaloric effects of $Gd_{65-x}RE_xFe_{20}Al_{15}$ ($x=0-20$; RE=Tb, Dy, Ho, and Er) ribbons, *J. Appl. Phys.* 109 (2011), 07A933.
- L. Liang, X. Hui, G.L. Chen, Thermal stability and magnetocaloric properties of $GdDyAlCo$ bulk metallic glasses, *Mater. Sci. Eng. B Solid.* 147 (2008) 13–18.
- Q. Luo, D.Q. Zhao, M.X. Pan, W.H. Wang, Magnetocaloric effect in Gd-based bulk metallic glasses, *Appl. Phys. Lett.* 89 (2006), 081914.
- A. Takeuchi, A. Inoue, Classification of bulk metallic glasses by atomic size difference, heat of mixing and period of constituent elements and its application to characterization of the main alloying element, *Mater. Trans.* 46 (2005) 2817–2829.
- M. Weinert, R.E. Watson, Hybridization-induced band gaps in transition-metal aluminides, *Phys. Rev. B* 58 (1998) 9732–9740.
- Z.H. Liu, Y.J. Zhang, E.K. Liu, G.D. Liu, X.Q. Ma, G.H. Wu, Role of d-d and p-d hybridization in CoTi-based magnetic semiconductors with 21 and 26 valence electrons, *J. Phys. Appl. Phys.* 48 (32) (2015) 325001.
- C.C. Yuan, X. Shen, J. Cui, L. Gu, R.C. Yu, X.K. Xi, Atomic and electronic structures of Zr-(Co,Ni,Cu)-Al metallic glasses, *Appl. Phys. Lett.* 101 (2) (2012), 021902.
- D. van der Marel, G.A. Sawatzky, Electron-electron interaction and localization in d and f transition metals, *Phys. Rev. B* 37 (18) (1988) 10674–10684.
- R. Jullien, B. Coqblin, Study of d-f hybridization in actinide metals and alloys, *Phys. Rev. B* 8 (11) (1973) 5263–5271.
- C.C. Yuan, F. Yang, X.K. Xi, C.L. Shi, D. Holland-Moritz, M.Z. Li, Hu, B.L. Shen, X.L. Wang, A. Meyer, W.H. Wang, Impact of hybridization on metallic-glass formation and design, *Mater. Today* (2019), <https://doi.org/10.1016/j.mat-tod.2019.06.001> in press.
- Y. Henry, K. Ounadjela, Evidence for a direct d-d hybridization mechanism for the interlayer exchange coupling in epitaxial Co/Mn multilayers, *Phys. Rev. Lett.* 76 (11) (1996) 1944–1947.
- K.N.R. Taylor, M.I. Darby, *Physics of Rare Earth Solids*, Chapman and Hall, London, 1972.
- K.H.J. Buschow, Intermetallic compounds of rare-earth and 3d transition metals, *Rep. Prog. Phys.* 40 (1977) 1179.
- K.A. Gschneidner, V.K. Pecharsky, Magnetocaloric materials, *Annu. Rev. Mater. Sci.* 30 (2000) 387–429.
- F. Yuan, J. Du, B. Shen, Controllable spin-glass behavior and large magnetocaloric effect in Gd-Ni-Al bulk metallic glasses, *Appl. Phys. Lett.* 101 (2012), 032405.
- K.A. Gschneidner Jr., A.O. Pecharsky, V.K. Pecharsky, Low temperature cryocooler regenerator materials, 12th Int. Cryocooler Conf. (2002) 1–9.
- V. Franco, A. Conde, M.D. Kuz'min, J.M. Romero-Enrique, The magnetocaloric effect in materials with a second order phase transition: are T-C and T-peak necessarily coincident? *J. Appl. Phys.* 105 (2009), 07A917.
- V. Franco, J.S. Blazquez, A. Conde, Field dependence of the magnetocaloric effect in materials with a second order phase transition: a master curve for the magnetic entropy change, *Appl. Phys. Lett.* 89 (2006) 222512.
- P. Yu, N.Z. Zhang, Y.T. Cui, L. Wen, Z.Y. Zeng, L. Xia, Achieving an enhanced magneto-caloric effect by melt spinning a $Gd_{55}Co_{25}Al_{20}$ bulk metallic glass into amorphous ribbons, *J. Alloys Compd.* 655 (2016) 353–356.
- Q. Luo, W.H. Wang, Rare earth based bulk metallic glasses, *J. Non-Cryst. Solids* 355 (2009) 759–775.
- V. Franco, A. Conde, V. Provenzano, R.D. Shull, Scaling analysis of the magnetocaloric effect in $Gd_5Si_2Ge_{1-x}X_{0.1}$ (X=Al, Cu, Ga, Mn, Fe, Co), *J. Magn. Magn. Mater.* 322 (2010) 218–223.

- [43] F. Hu, C. Yuan, Q. Luo, W. Yang, B. Shen, Effects of Ho addition on thermal stability, thermoplastic deformation and magnetic properties of FeHoNbB bulk metallic glasses, *J. Alloys Compd.* 807 (2019) 151675.
- [44] J.W. Li, W.M. Yang, D. Estéve, G.X. Chen, W.G. Zhao, Q.K. Man, Y.Y. Zhao, Z.D. Zhang, B.L. Shen, Thermal stability, magnetic and mechanical properties of Fe-Dy-B-Nb bulk metallic glasses with high glass-forming ability, *Intermetallics* 46 (2014) 85–90.
- [45] J.F. Herbst, J.J. Croat, Magnetization of RFe₃ intermetallic compounds: molecular field theory analysis, *J. Appl. Phys.* 53 (1982) 4304–4308.
- [46] J. Huo, L. Huo, H. Men, X. Wang, A. Inoue, J. Wang, C. Chang, R.-W. Li, The magnetocaloric effect of Gd-Tb-Dy-Al-M (M = Fe, Co and Ni) high-entropy bulk metallic glasses, *Intermetallics* 58 (2015) 31–35.
- [47] L. Liang, X. Hui, Y. Wu, G.L. Chen, Large magnetocaloric effect in Gd₃₆Y₂₀Al₂₄Co₂₀ bulk metallic glass, *J. Alloys Compd.* 457 (2008) 541–544.